ISSN 1726-5479

SENSORS & TRANSDUCERS

3/12 vol. 138

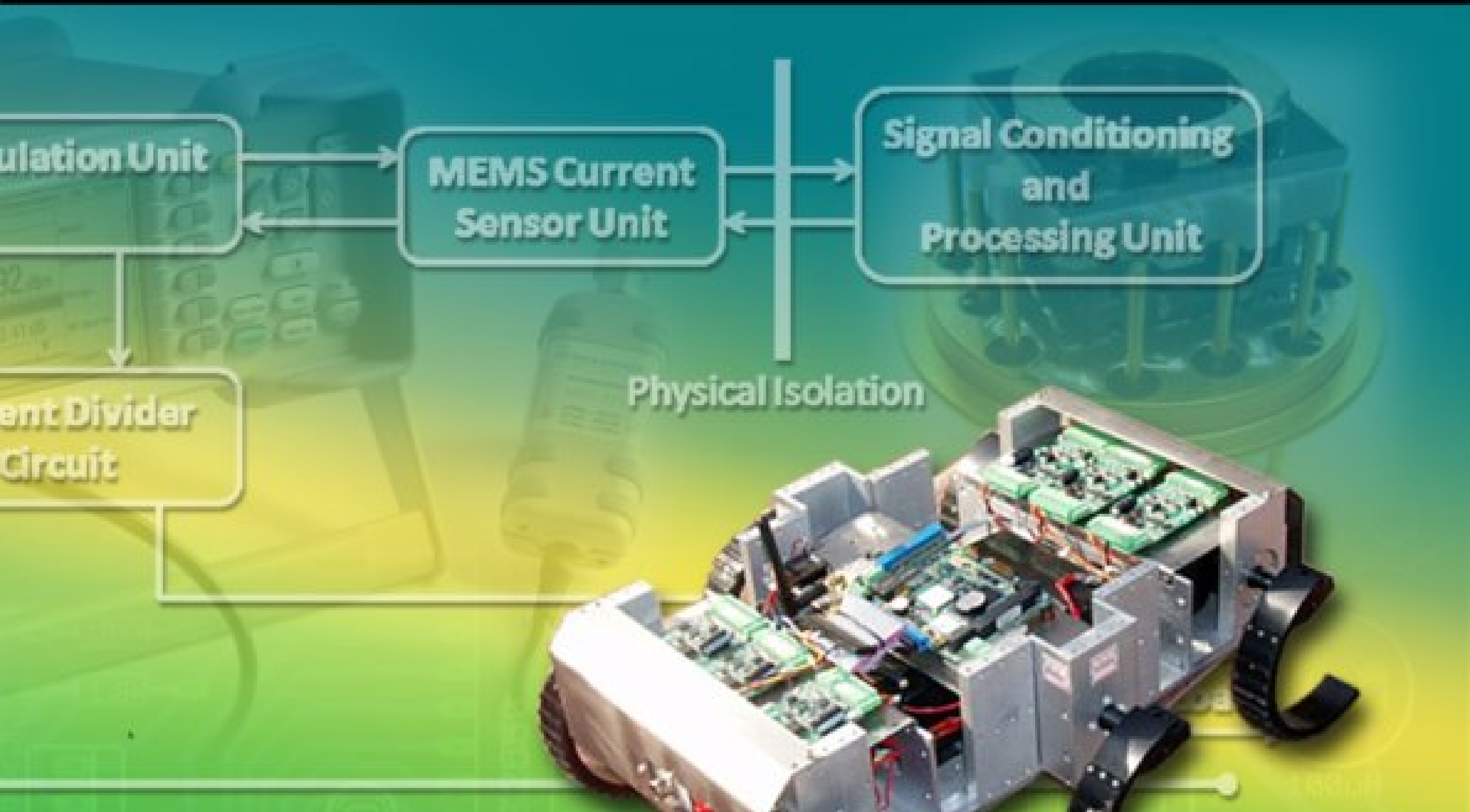

Smart Sensors and Intelligent Sensor Systems

International Frequency Sensor Association Publishing

Sensors & Transducers

Volume 138, Issue 3, March 2012 **www.sensorsportal.com** **ISSN 1726-5479**

Sensors & Transducers Journal (ISSN 1726-5479) is a peer review international journal published monthly online by International Frequency Sensor Association (IFSA).
Available in electronic and on CD.

Contents

Volume 138
Issue 3
March 2012

www.sensorsportal.com

ISSN 1726-5479

Research Articles

Automotive Pressure Sensor (White Paper)
Ninghai Sendo International Trading Co., Ltd. 1

A Novel MEMS Based Current Sensor Design for Smart Grid Applications
A. Venkateswaran, A. Amalin Prince........ 3

Application of Frequency-Domain Integral Algorithm to the Processing of Sport Signals Based on MTi Sensor
Qian Yu, Yunjian Ge, Tingting Ma, Zeyuan Lu........ 14

A Compact X-ray Spectrometer Using Silicon Drift Detector
M. Shanmugam, Y. B. Acharya, V. Mishra, P. N. Patel, S. K. Goyal 22

Virtual Instrumentation with Application in Multiaxial Extensometric Force Platform
André Guimarães Oliveira and Alexandre Balbinot........ 35

Measurement of Bubble Flow in Liquid Using Optical Tomography
Naizatul Shima Mohd Fadzil, Siti Zarina Mohd Muji, Ruzairi Abdul Rahim, Yusri Mohd Yunus, Salinda Bunyamin, Shafishuaza Sahlan, Nor Muzakkir Nor Ayob........ 50

Evaluation of Online Strain Monitoring of Concrete/Steel Structures - Laboratory and Field Studies
M. S. Karthikeyan, A. K. Parande, K. Kumar, R. Jeyaram, N. Palaniswamy, A. Sivashanmugam, R. H. Suresh Bapu, K. Lakshmibarani and C. Ponraj........ 59

Applications of Angular Measurement Using Hit or Miss Transform
N. S. Abinaya, V. R. Priya and S. Rakesh Kumar........ 71

Design of Cursor Magnets on the Wiedemann Effect in Magnetostrictive Linear Position Sensors
Yong-Jie Zhang, Chun-Feng L. V., Jin-Feng Yang, Wei-Wen Liu, Hui Zhao........ 80

Data Acquisition Latency in Dynamic Localization: A Weighted Least Squares Approach
Mohammad Amin Rahimian, Shinji Ohyama 88

Stability Analysis and Design of PI Controller Using Kharitnov Polynomial for Rotary Inverted Pendulum
Jim George, Bipin Krishna, V. I. George, Shreesha C., Mukund Kumar Menon 104

Energy Harvesting Via Pyroelectric Transducer
Ashok Batra, Sudip Bhattacharjee, Aswith Chilvery and Jason Stephens........ 114

Dynamic Control of Hexapod Robot Based on Plantar Pressure Sensor
Yong FENG, Yunjian GE, Yan Huang........ 122

Study on Speed Adaptation Control for a Gait Rehabilitation Training Robot
Yongjiu Liu, Buyun Wang, Guangbin Zhang, Tingting Ma, Feng Shuang and Quanjun Song.. 132

Stochastic Filters for Mobile Robot SLAM Problems - A Review
K. Ramkumar, N. S. Manigandan... 141

Authors are encouraged to submit article in MS Word (doc) and Acrobat (pdf) formats by e-mail: editor@sensorsportal.com
Please visit journal's webpage with preparation instructions: http://www.sensorsportal.com/HTML/DIGEST/Submition.htm

International Frequency Sensor Association (IFSA).

Sensors & Transducers Journal, Vol. 138, Issue 3, March 2012, pp. 35-49

www.sensorsportal.com

Sensors & Transducers

ISSN 1726-5479

http://www.sensorsportal.com

Virtual Instrumentation with Application in Multiaxial Extensometric Force Platform

André Guimarães OLIVEIRA and Alexandre BALBINOT
Instrumentation Laboratory (IEE)
Electrical Engineering Department (DELET)
Federal University of Rio Grande do Sul (UFRGS) – Avenue Osvaldo Aranha,
103 - 203, Porto Alegre, 90035-190, Brazil
Tel.: +550215133084440
E-mail: paladinox@gmail.com, alexandre.balbinot@ufrgs.br

Received: 17 January 2012 /Accepted: 20 March 2012 /Published: 31 March 2012

Abstract: This paper presents the development of an experimental system to measure the forces involved in a 3D force platform that supports up to 1000N in its vertical axis. Experimental data were compared with simulated data using finite elements method (FEM). Data acquisition and processing were performed using LabView software with USB6008 data acquisition board from National Instruments. Results showed a linearity error of 0.49 % on the vertical axis, revealing the smooth functioning of the system. Found deformations in the load cells were compared with the simulated model, showing a difference of 5.8 % at most. *Copyright © 2012 IFSA.*

Keywords: Load cell, Force platform, Strain-gages, LabVIEW.

1. Introduction

Simple everyday activities use correct balance and body orientation to maintain correct posture. When walking, running, lying down, and even stop standing, the muscle system is at all times correcting efforts to maintain balance. Even when an individual is standing still, oscillations occur so that the muscle forces control the human body gravity center. Arrangement of relative angles of all joints involved in the equilibrium position can be called posture [1].

The human gait is a complex phenomenon not usually described analytically, because there are a large number of variables to be studied. Thus, the human gait analysis through the soil reaction, stepped reaction, among others simplify the study process and makes possible data acquisition for its characterization.

This paper presents the development and simulations of a square shaped force platform, coupled to four load cells made of AISI304 stainless steel [2], arranged on a rigid base of ABNT1020 carbon steel [3]. Experimental data are obtained from extensometers cemented on load cells. To facilitate these data interpretation, a computational tool for analysis was developed using LabView software from National Instruments. The force platform and the load cells are analyzed through simulations in SolidWorks program and through experimental procedures described in this paper.

2. Basic Concepts

Faced with the range of sensors and transducers for researches and for automotive and industrial applications, the load cells are considered one of the most important transducers in the market. Basically, a load cell measures deformations caused by different kinds of forces [4]. The main reasons for using load cells are related to its high response fidelity, low cost, small size (even for heavy loads' applications), and to allow dynamic measurements.

Typically, in the load cells, in which the elastic element undergoes small deformations, the extensometer is the sensor normally used. When the elastic element undergoes a large deformation, we look usually for a displacement sensor/transducer (inductive, capacitive, or resistive), which gives a signal that translates the deformation produced by applied load [5]. Load cells are usually classified according to configuration type of its elastic element. The most common load cells are column, beam, and embedded ring-type [5]. The ring-type load cell has geometry in order to isolate efforts in the horizontal plane, allowing a three-dimensional analysis, when it is combined with load cells. It has similar configuration of the load cell used in this work.

Fig. 1 shows a typical transduction chain for load cells. In extensometers of metal film, its electrical resistance parameter is changed by mechanical characteristics, because some deformation occurs, when a force is applied to an object. Strain (ε) is defined as deformation amount per object's length unit and is determined by dividing the total deformation of the original length (Δl) by object's original length (l_o), represented in Equation (1):

$$\varepsilon = \frac{\Delta l}{l_o} \tag{1}$$

The relationships that describe the typical behavior of extensometer are given by equation (2):

$$GF = \frac{\Delta R / R}{\Delta l / l_o} = \frac{\Delta R / R}{\varepsilon} \tag{2}$$

in which GF is the gage factor, ΔR is the change in electrical resistance according to the conductor deformation, R is the electrical initial resistance, Δl is the length change, l_0 is the initial length, and ε is the deformation per length unit. Each material type for extensometer has certain characteristics, such as gage factor (GF), resistance (R), temperature coefficient, and stability. Typical materials used to manufacture the extensometers are Constantan (copper-nickel alloy), Nichrome (nickel-chromium alloy), platinum alloys, isoelastic alloys (nickel-iron alloy), laminas or semiconductor materials, and the most common are copper-nickel alloys and nickel-chromium [6].

Fig. 1. Typical transduction chain for load cells.

3. Experimental Methodology

Fig. 2 shows the blocks diagram of the developed system. The force platform was developed to support an adult human, standing or moving. To indicate the applied forces, four load cells for 3D measurement were built, based on Bagesteiro [7] and Urquiza [8] studies.

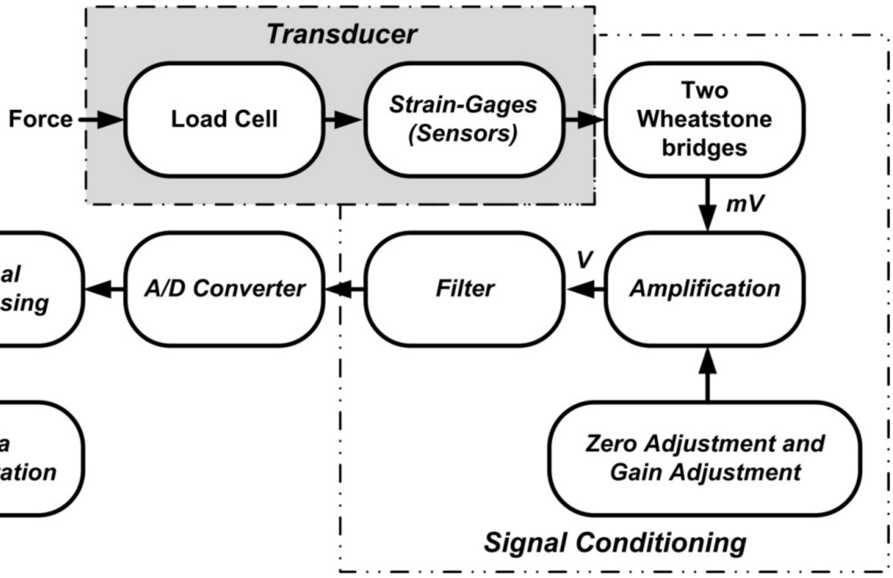

Fig. 2. Blocks diagram of the experimental system.

The load cells disposition aims to isolate forces, so the 3D effect can be measured by adding the contributions of each load cell. The upper surface transmits the effort to load cells, while the bottom surface serves as support base required by other platform components that, besides allowing the setting of load cells, is considered in this work a rigid base [7, 8].

Used materials seek to optimize its function. Due to the need for a rigid base and mainly due to costs, ABNT 1020 carbon steel plate [3] was adopted. But the top plate should be softer to transfer forces applied on its surface; for that, the used material was Naval aluminum 5052 F [9]. Both load cells and support bearings were produced with the same material, i.e., stainless steel AISI 304 alloy [2]. Each load cell has eight extensometers distributed into two sets that form two complete Wheatstone bridges, as shown in Fig. 3.

Output values of each Wheatstone bridge, ΔV_H and ΔV_V, represent the horizontal and vertical output voltage, respectively. The strain-gages used in this work belong to PA-06-125A-350-L model, with terminals soldered by copper, self-temperature compensation for steel, 2.13-gage factor, and 350 Ω resistance. The strain-gages were bonded with cyanoacrylate glue, after the surface being lightly sanded and cleaned with isopropyl alcohol to remove some impurities and possible fat.

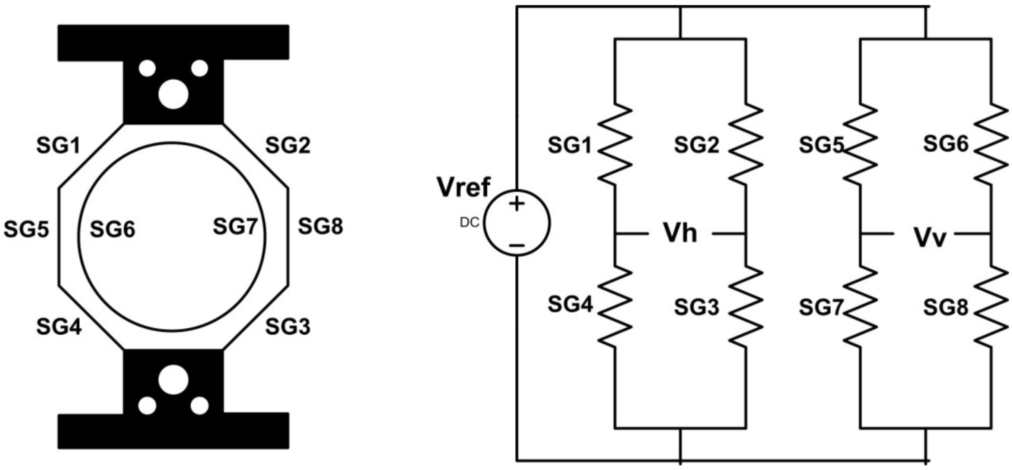

Fig. 3. Strain-gages disposition (red) on the load cell and two Wheatstone bridges configuration.

3.1. Force Platform Simulation

For analysis in SolidWorks software, the platform was designed according to its dimensions and properties, considering the shape and materials used for construction the load cell. Data on elastic modulus, Poisson's ratio, shear modulus, tensile, compressive, and yield strength are obtained from simulator database. The load cells' arrangement makes possible to isolate the forces in 3D axes [7, 8]. Figs. 4 (a) and (b) show the platform in simulation procedure.

The next steps are the application of mounts and add the involved forces so that they can resemble the situation in which the experimental platform will be submitted. Fig. 4 (c) shows the forces applied to the force platform (represented by red at the top of the force platform); and the mount applied to platform is represented by green (base of the force platform).

For dynamic study of the system, SolidWorks software considers the structure and its materials, determining their vibration modes. After obtaining these frequencies, it is possible to determine whether the system will find some event, situation in which the system can be subjected and would become unstable. A load with oscillations in the range of certain vibration modes could damage the force platform, significantly interfering in the measures, in the linear system behavior, and in the structural health of the own platform. Thus, the use of platform should avoid this behavior type.

The procedure for dynamic analysis requires the same base of static test and the mount is taken again as reference. Once completed the design, the mount, and the materials characterization, the analysis in the frequency domain is accessed through the module of dynamic simulation test, which will provide the data for each frequency and corresponding vibration modes of the simulation.

3.2. Chain of Proposed Measure

The force applied on the force platform leads to the load cell deformation, promoting changes in the extensometer resistance. Thus, through proper conditioning, it is possible to monitor electrically the deformation by gain and filtering stages of the corresponding interest signal. To facilitate the understanding of all the involved essential steps, Fig. 5 shows the measurement chain proposed in this paper.

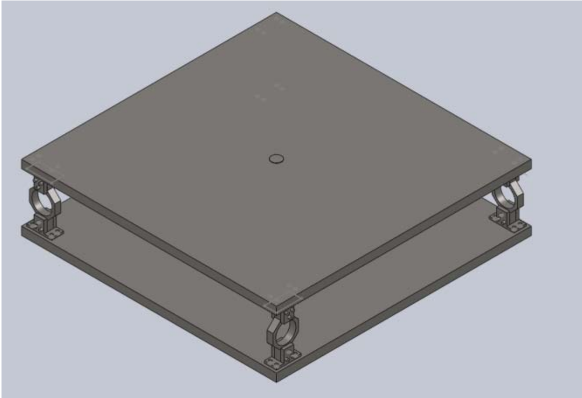

(a)

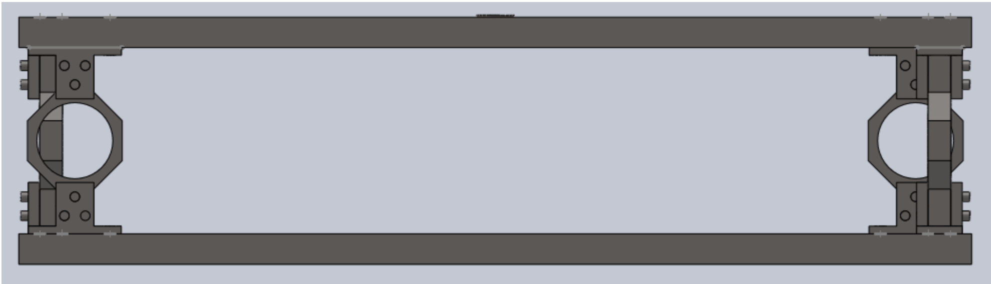

(b)

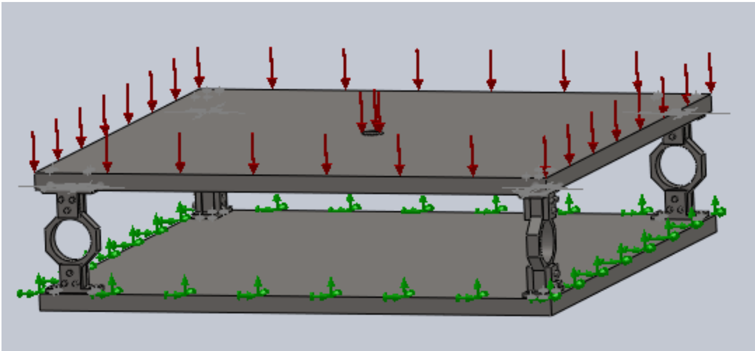

(c)

Fig. 4. (a) Isometric view; (b) Front view of the force platform; (c) Indication of the force application and the mounts on the force platform.

The planned load is of 1000 N, whose value is shown at the beginning of the measuring chain. According to simulation data, deformation of 50 με in the load cell and a change of approximately 100 μΩ in the extensometer resistance are expected. This resistance variation causes a potential difference of about 1 mV in Wheatstone bridge, which comes to a full scale of 10 V, after the two gain stages. This signal is then digitized by ADC board and represented graphically in the software that was developed.

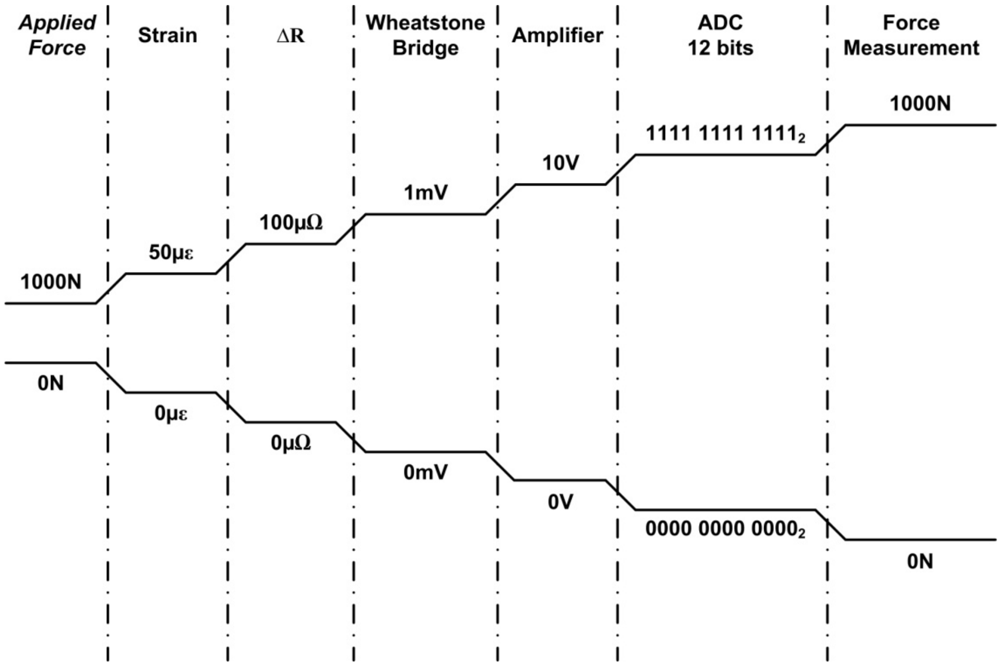

Fig. 5. Chain of the proposed measure.

3.3. Conditioning and Data Acquisition

The system output voltage should be directly proportional to circuit voltage. Therefore, it is necessary to ensure that supply voltage of Wheatstone bridge is stable, in order to obtain a reliable measure and thus minimize possible errors due to poor quality of power supply. Based on this criterion and on the developing cost of a stable system, CI REF02 was chosen to be used, thus enabling a constant and independent power source (in its work range). With an operational amplifier and a transistor, one configuration was developed to obtain a power supply with 5.0 V reference and current capacity of 1.5 A (Fig. 6 (a)). There is a multi-turn potentiometer (P1) connected to Vs and GND with its central terminating attached to a resistor in series and to one arm of the Wheatstone bridge (Fig. 6 (b)). Thus, zero adjustment is performed to balance the Wheatstone bridge (an individual circuit for each one of the bridges).

Using a constant power source, the next step is the development of the signal amplification from the Wheatstone bridge. The use of instrumentation amplifiers is interesting, since the circuit operates in differential mode and should have low noises emission. CI INA126 was chosen and two amplification stages were needed (Fig. 6 (c)).

One analog Butterworth low-pass filter was developed with two poles and 12 db/octave per stage. Its cutoff frequency should be determined in accordance to the phenomenon being measured, in this case, with a frequency range below 10 Hz.

After filtering through two stages, the signal was acquired by DAQ USB 6008 data acquisition board at a rate of 1,000 samples per second and resolution of 12 bits. Later, the data were processed and displayed by LabView. It is important to note that a shielded cable was used for connecting the extensometers to conditioning plates for minimizing noises. Eight input channels of the ADC board were used, namely, four vertical channels and four horizontal channels. It should be noted that, besides the filter setting at the conditioning board, a digital 3rd order Butterworth low-pass filter was also implemented.

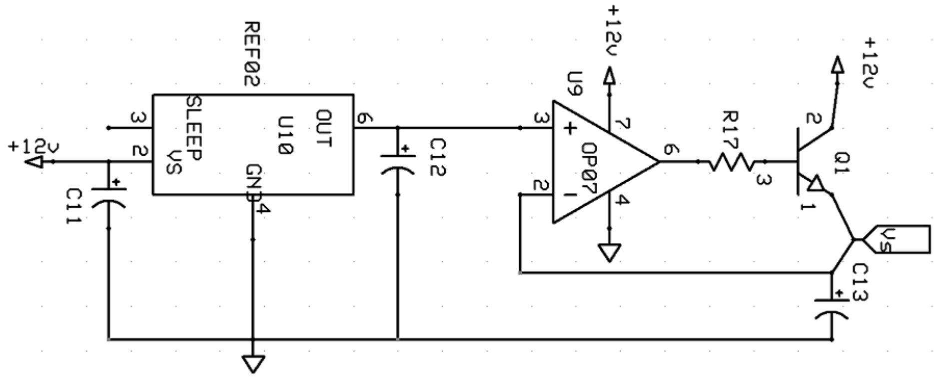

(a)

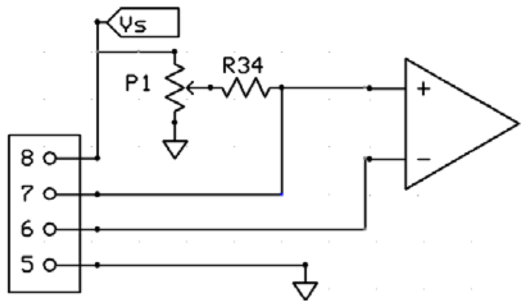

(b)

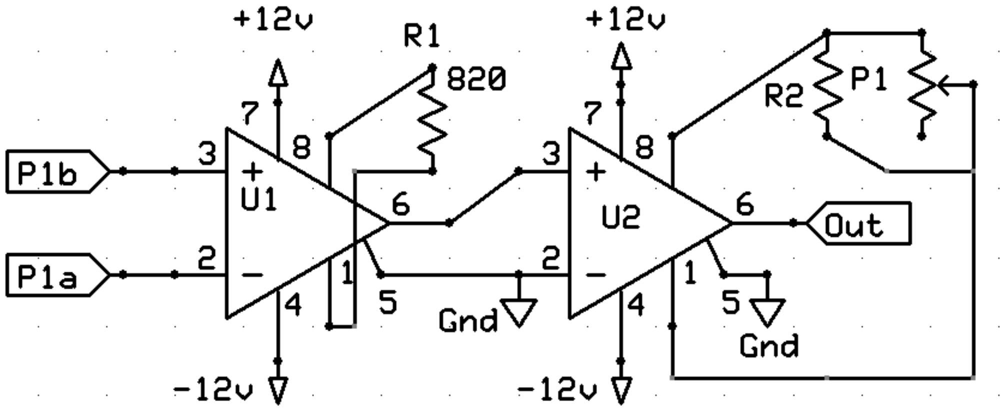

(c)

Fig. 6. (a) Constant power source; (b) Zero adjustment; (c) Gain stage.

Each channel is treated separately by adjustable gain and by mathematical operations that are required for information display. Graphs show the location of the resultant force from z (pressure center), x, and y-axes, the value, and time. Fig. 7 shows the human-machine interface of the developed system. After acquisition, each data channel is treated separately, i.e., initially each signal is adjusted by an adjustable gain and then mathematical operations are performed. Thus, the force components of each load cell are combined in z vertical axis as in x and y horizontal axes. To obtain the force applied to z-axis, the four components that have individual gain adjustment are added by an adder block. The mass is calculated by simple multiplication of a fixed value (gravity acceleration). After these mathematical operations, the data are graphically displayed in the interface (Fig. 7).

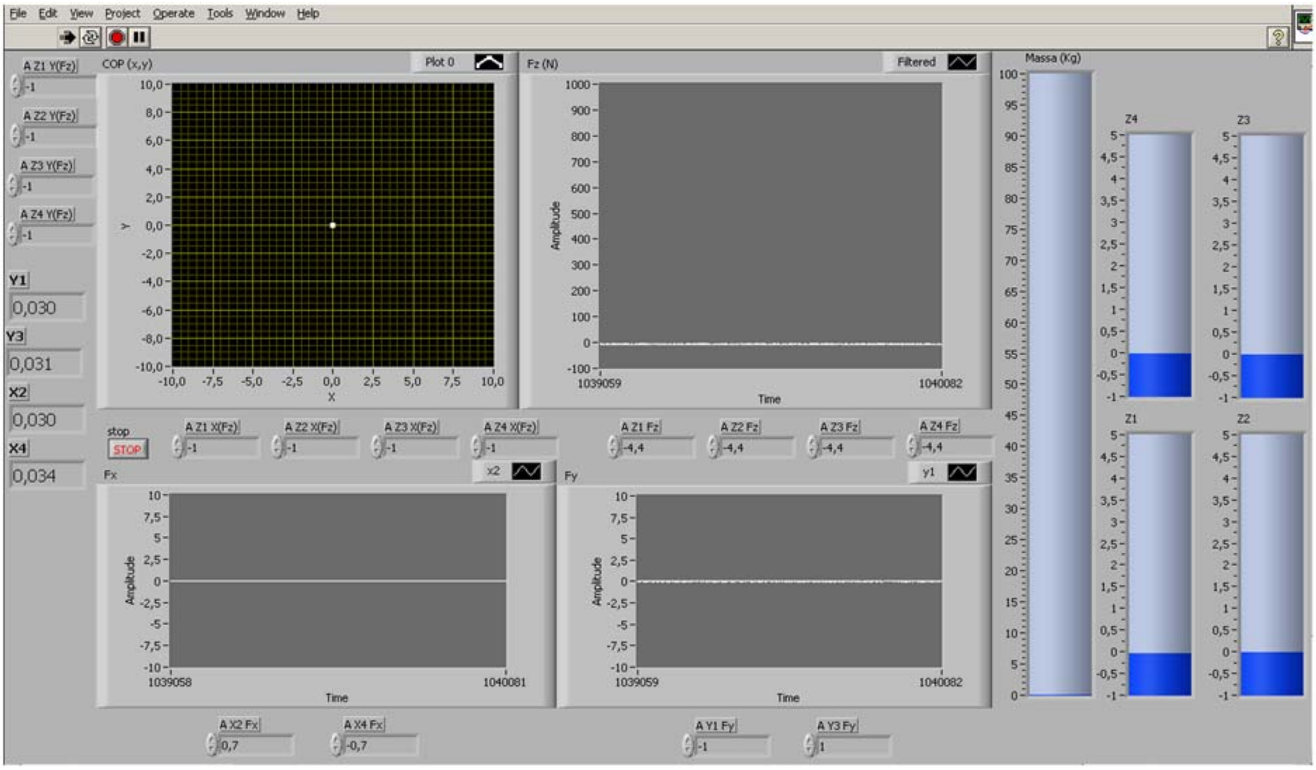

Fig. 7. Human-machine developed interface.

3.4. Calibration Procedures

The z-axis static calibration was performed by applying different pattern weights. Dynamic test was performed using the method called impact. For it, one DeltaTron accelerometer (model 4520 from Bruel & Kjaer) was positioned in the center of the force platform and an impact was generated using a rubber mallet. For acquisition and conditioning of accelerometer signal, NI SCXI conditioning system of the National Instruments was used. At the impact moment, the data were acquired and analyzed in the frequency domain by FFT (Fast Fourier Transform) showing the piece resonances.

The proposed system has eight full Wheatstone bridges, namely, four to analyze the z-axis of coordinates, two for the y-axis, and two for x-axis.

Thus, the gain adjustment of each bridge along with its zero adjustment through the proposed potentiometers compose the conditioning system. The output signal of each one of the eight bridges is acquired and processed digitally.

The static calibration was performed by adding standard weights on the platform surface. After the correct setting to zero, the gain was adjusted so that all load cells have equal contribution in shaping the forces resultant. In addition to vertical setting (z-axis), the reference points of horizontal axes must observe the same requirement, and each Wheatstone bridge should contribute in the same manner and intensity for effects in both the x-axis and y-axis.

The experimental data were compared with simulations to verify their consistency. The software developed in LabView allowed equalizing the contributions of each one of the eight Wheatstone bridges from the force platform by adjustable multiplication to each channel, showed by Fig. 7. After this adjustment, a resultant force is shown by values from load cells; the sum and difference of the axes determine the pressure center (PC) through z-axis components.

4. Results and Discussions

4.1. Simulations

Fig. 8 shows the simulated result of static deformation during load application of 1000 N at the force platform center. The points where the extensometers were glued reach deformation around 47 με values and are represented by red color. Fig. 9 shows the platform static displacement with application of maximum load (1000 N) at its center. It is possible to observe that the top plate has the largest displacement in the center, around 47 μm, generating a displacement of about 10 μm in the load cells. Static tensions are shown in Fig. 10. With this study, it is possible to determine the structure mechanical limits and verify that the mechanical stress is within the material limits. With the applied load, there is a maximum voltage of about 16 million N/m^2, and the yield strength of the load cell material is around 200 million N/m^2, providing a high safety factor against possible plastic deformations.

The vibration modes from dynamic simulation are presented in Table 1. As the simulation results in Fig. 11, the first vibration mode is located at 183.20 Hz, higher frequency than the signals to be measured with Hertz units. The software developed in LabView has 18 dB/octave Butterworth low-pass filter at 10 Hz tuned, because the interest frequencies are smaller than 5 Hz. It is noted that the support bearings (Fig. 10) are subjected to voltages about five times lower than the ring of the load cell. Considering they have the same material of ring, there is not an obstruction in the application of the rated load of 1000N in relation to deformation problems or bearings flow.

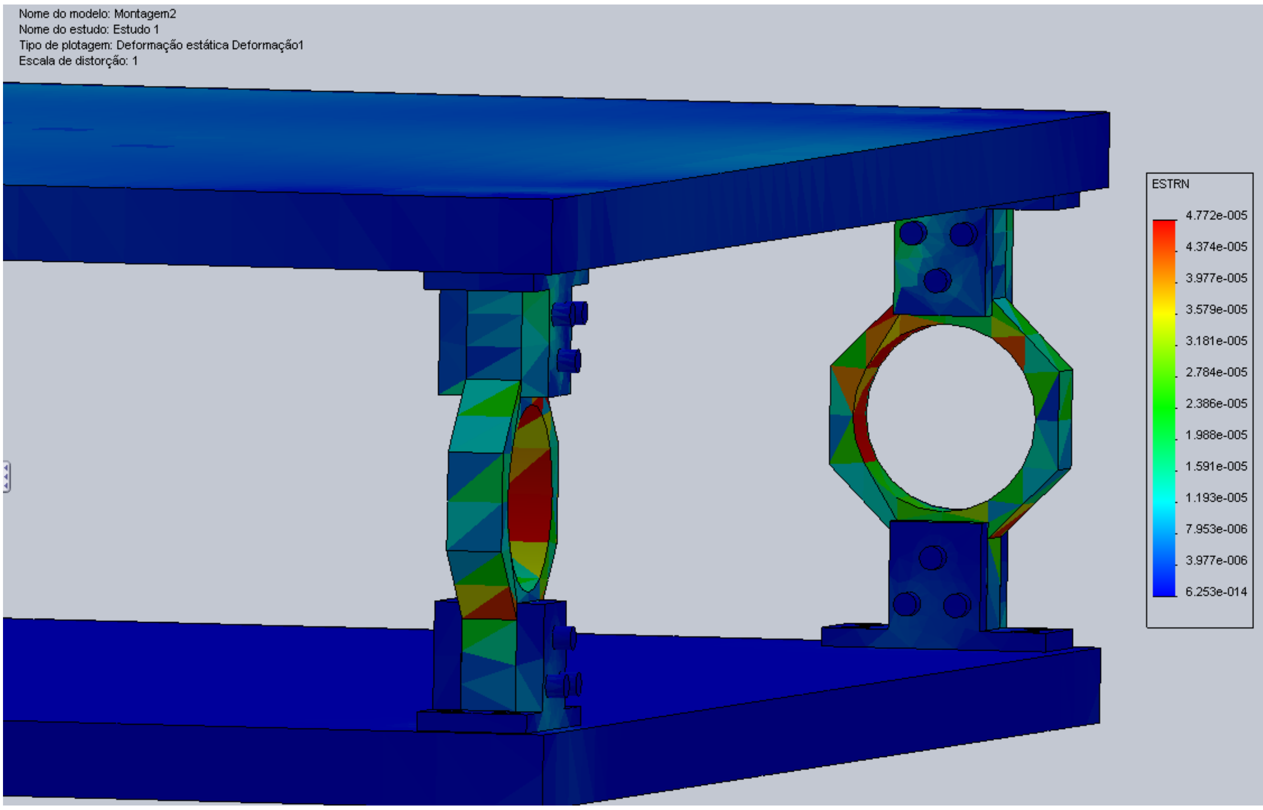

Fig. 8. Static deformation - ε scale**.**

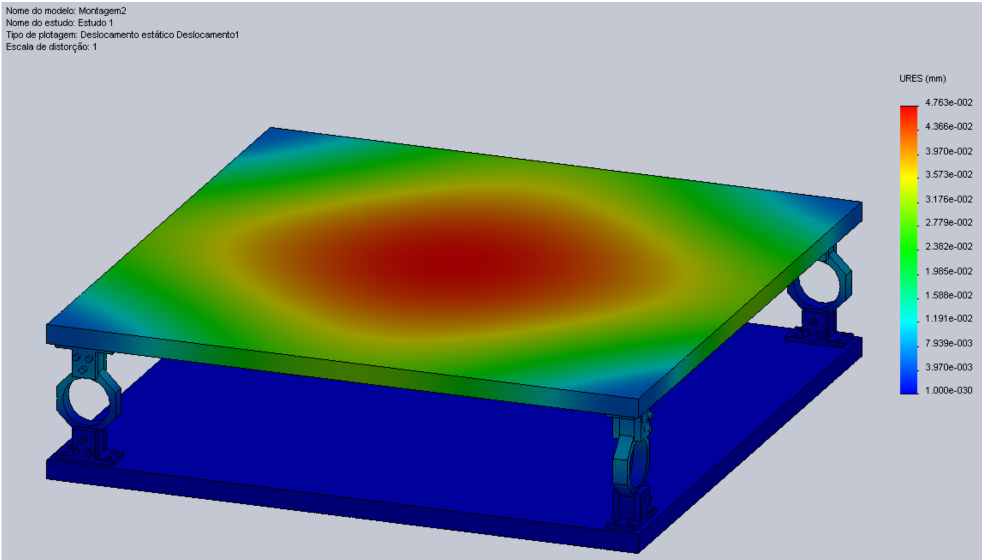

Fig. 9. Static Displacement - scale in millimeters.

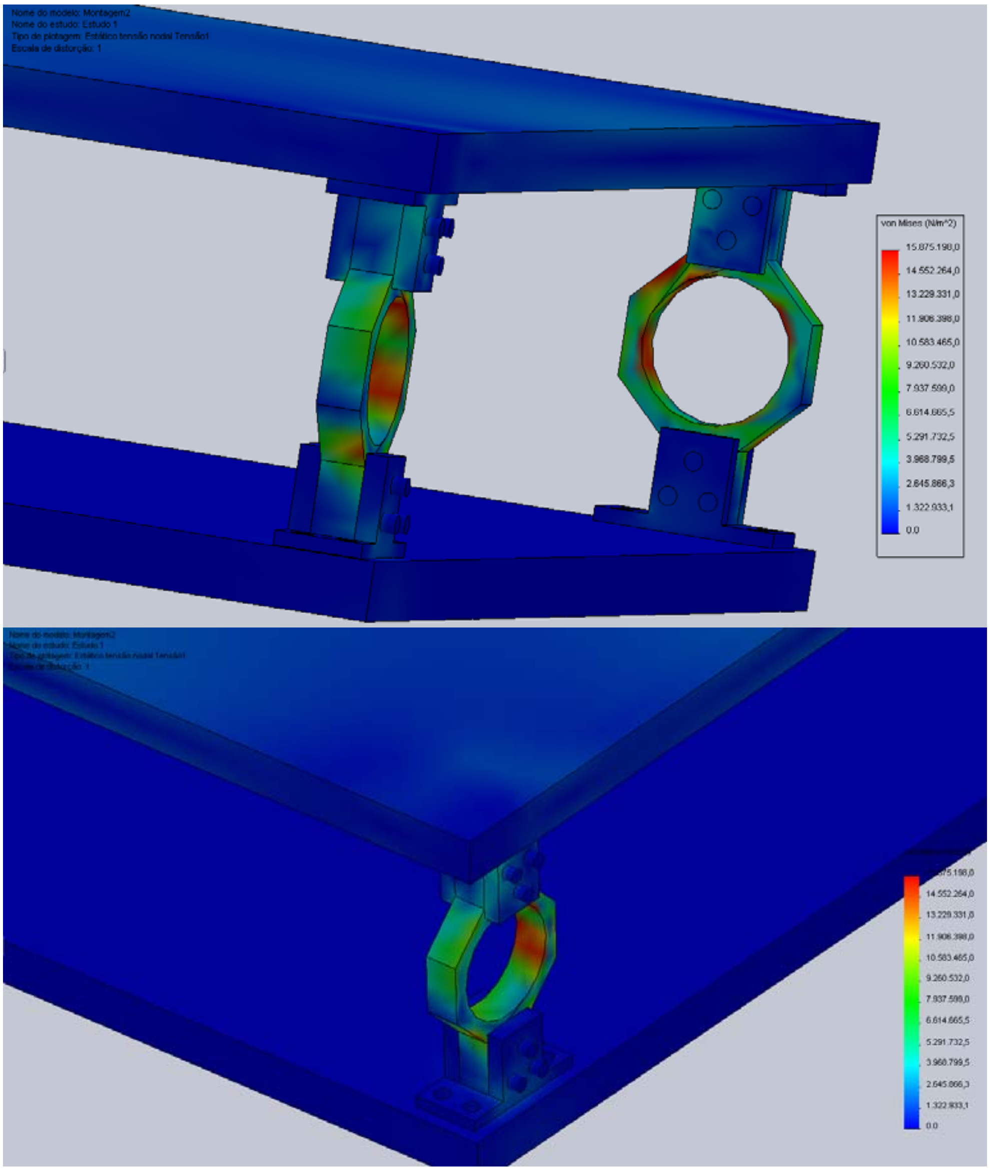

Fig. 10. Static Voltages - N/m^2 scale.

Table 1. Dynamic simulation results - vibration modes.

Modes	Frequency [Hz]
1	183.20
5	348.99

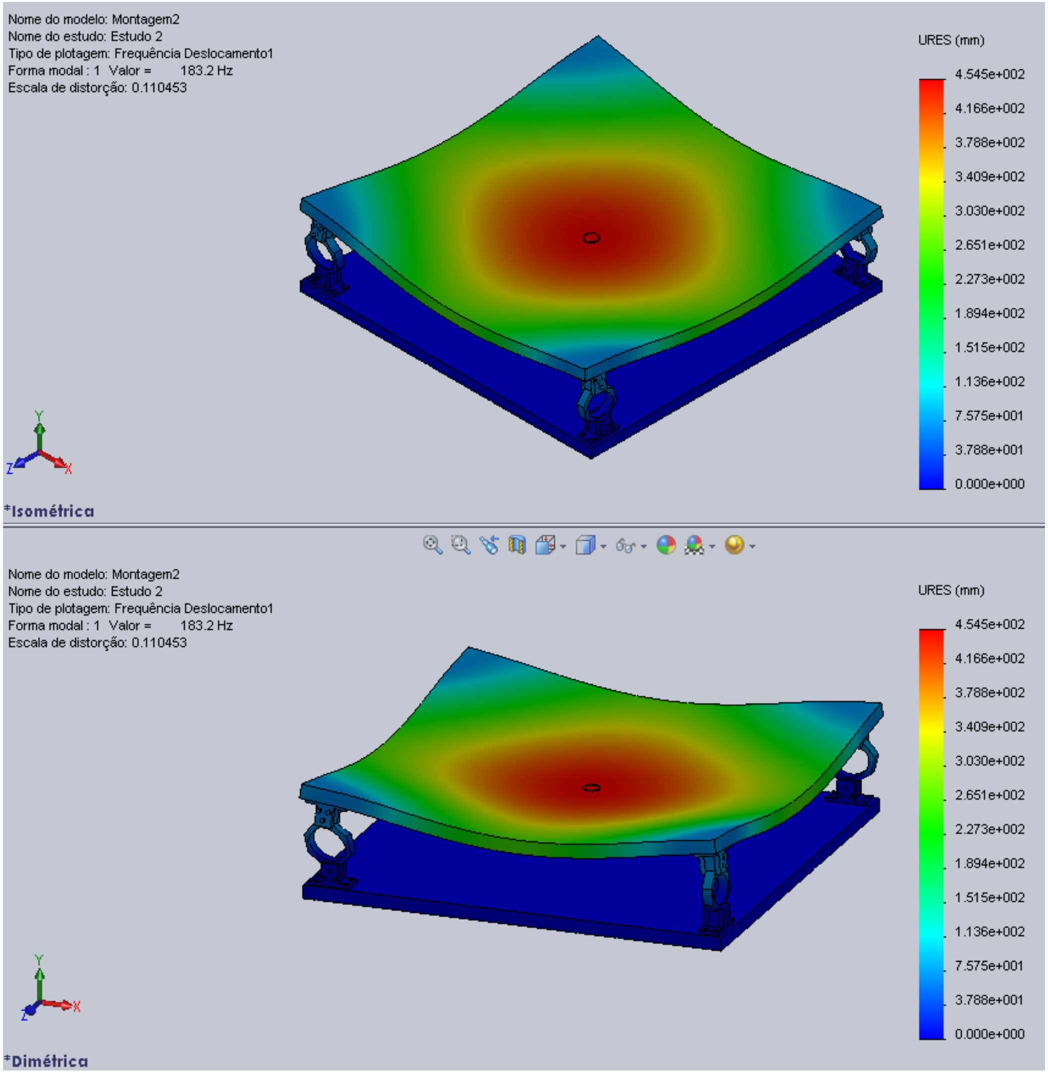

Fig. 11. Modal form 1 - 183.20 Hz.

4.2. Experimental Results

For calibration purpose, data were obtained from the platform after zeroing the output of each channel of the system. The four channels of the z-axis were measured simultaneously by four ICEL MD2000 multimeters in the scale of 20 V after standard weights application in the force platform center. The arithmetic mean of these data was calculated and used to plot the graph of Fig. 12, which presents the experimental calibration curve of the platform on z-axis (parallel to gravity) with linearity error of 0.49 %.

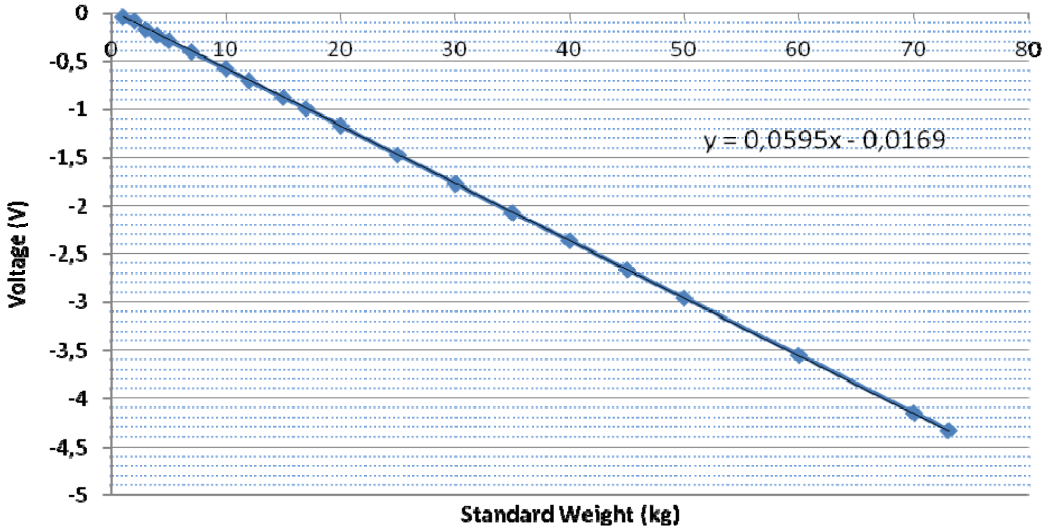

Fig. 12. Experimental calibration curve of the force platform - z-axis.

Individual calibration of each load cell in z-axis was also performed through test with standard weights applied directly on top of each load cell (in platform corners). So, it is possible to analyze and compare the performance of each individual load cell. In this case, values in the four load cells were summed to obtain normalization in comparison to individual cell. According to experimental data, the sensitivity of the linearized system can be approximately given by Equations (3) to (5) in $^{V}/_{kg}$:

$$axis\_x = 0,54 \times m - 0,23 \tag{3}$$

$$axis\_y = 0,44 \times m + 0,11 \tag{4}$$

$$axis\_z = 0,059 \times m - 0,017 \tag{5}$$

in which *m* is the mass applied to each axis. The linearity errors found in all axes were 1.2 % for x-axis, 1.5% for y-axis, and 0.49 % for z-axis. This difference is due to the difficulty of positioning the standard weights to determine the x and y-axes.

The conditioning has enabled to obtain data consistent with project needs and for data acquisition. For conditioning the extensometers signal, two amplification stages with INA126 integrated circuit (instrumentation amplifier) were used with gain set at 100 for each stage. These gain stages provided an output voltage in the range of -10 V to 10 V, compatible with USB 6008 acquisition board.

The dynamic experimental acquisition was performed using the impact method with a commercial accelerometer sensor (described in Section 3.5). These data were acquired at a rate of 1000 samples per second with 12 bits resolution. The time curve is shown in Fig. 13 (a) and the corresponding FFT in Fig. 13 (b), after the impact on the force platform. Table 2 compares the experimental data with the simulated data, which are consistent. The values found in both the experimental testing as in the simulation do not present risk for platform usage, in which the involved frequencies are of Hertz units.

Table 2. Comparison of the simulated and experimental vibration modes.

Vibration Modes	Simulation [Hz]	Experimental [Hz]	Difference [Hz]
1	183	158	25
5	349	323	26

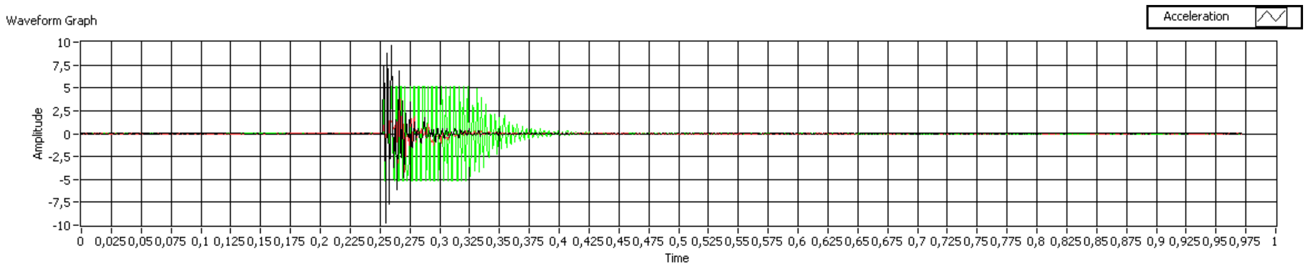

(a)

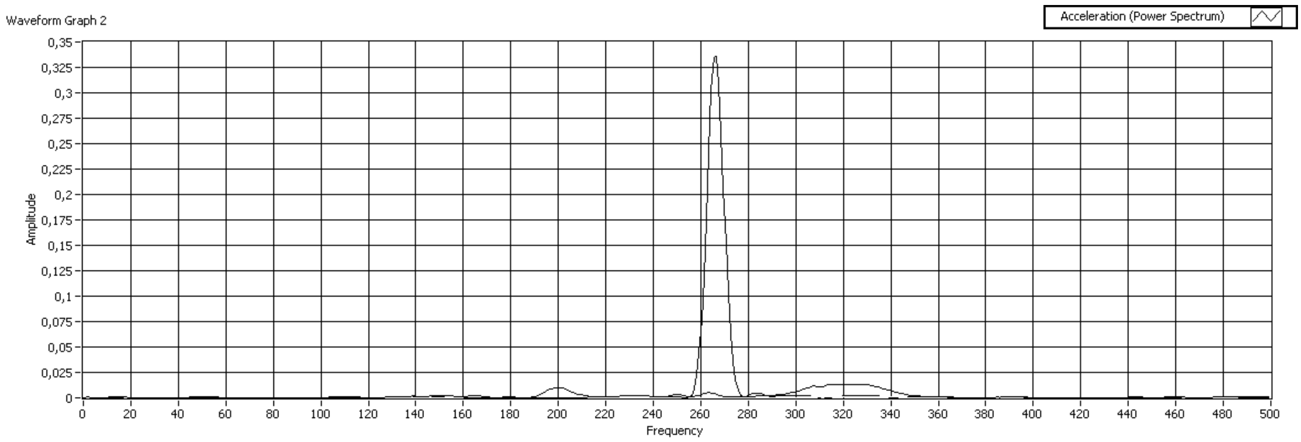

(b)

Fig. 13. (a) Dynamic test in function over time (z-axis in green); (b) The corresponding FFT.

4.3. Test on the Force Platform

After platform calibration and dynamic tests, one volunteer took the platform for testing purposes (Fig. 14). Then, the platform response was evaluated and compared with the calibration values for validation. In addition to resulting force on z-axis, the pressure center (PC) and forces in x and y-axes were evaluated. Fig. 14 shows the subject positioning and the values from software at the test moment.

(a)

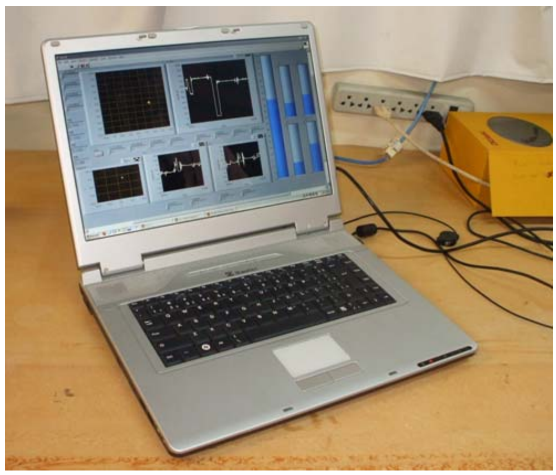

(b)

Fig. 14. (a) Subject positioning on the force platform; (b) Reading the results during test.

For the simulated model, Fig. 15 shows the simulation results performed for the same load, namely, displacement of 5.7 µm at the ring top and deformation around 48.6 µm/m at the extensometer location. Experimentally, using the data, the deformation can be calculated by Equation (6):

$$v_o = A\frac{\Delta R}{R}V_{REF} = 10000 \times GF \times \varepsilon \times V_{REF} = 10000 \times 2,13 \times \varepsilon \times 5 \qquad (6)$$

considering that 250 N is approximately 25.4 kg and using the values average found in calibration for mass of up to 25 kg (Equations (7) and (8)):

$$v_o = 5{,}5 = 10000.2{,}13 \times \varepsilon \times 5 \qquad (7)$$

$$\varepsilon = \frac{51.6\mu m}{m} \qquad (8)$$

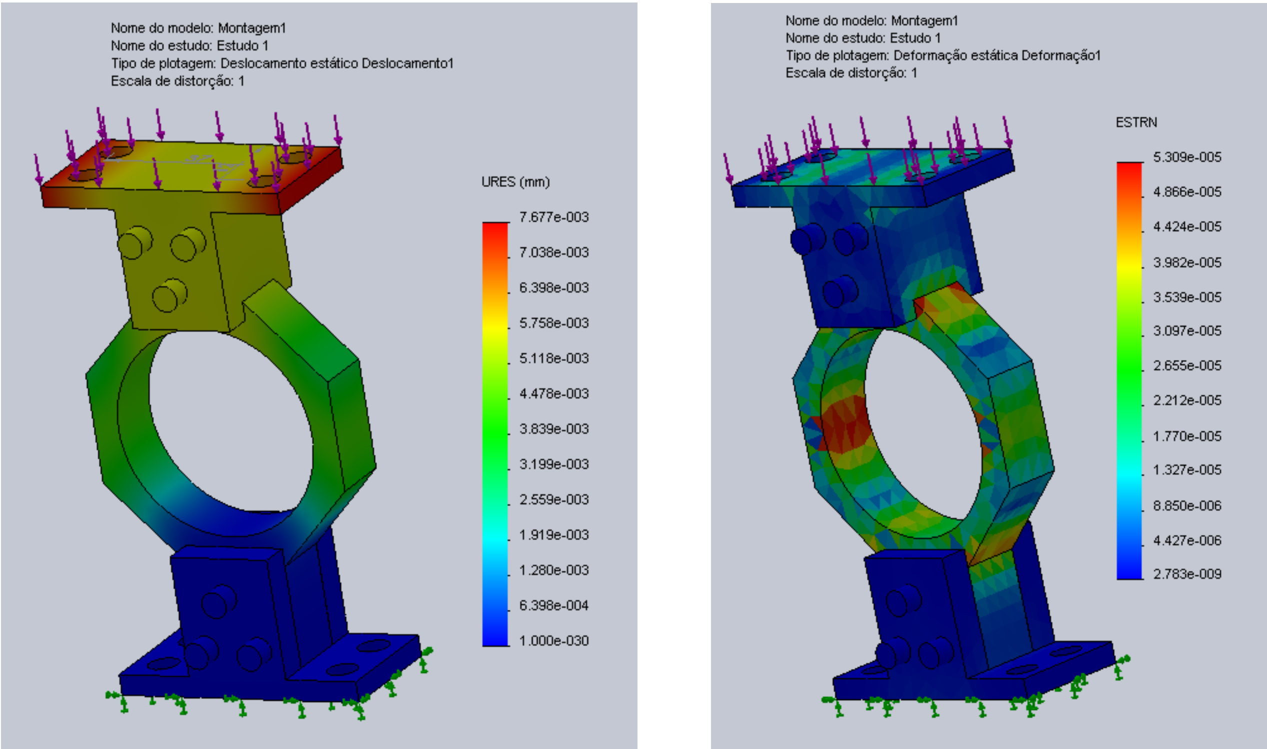

(a) (b)

Fig. 15. (a) Displacement of 5.7 µm at the ring top; (b) Deformation around 48.6 µm/m at the extensometer location.

Table 3 compares the results obtained through the three methods.

Table 3. Mathematical models comparison with the simulation and experimental data.

	Simulation	**Experimental**
Strain (µm/m)	48.6	51.6

Deformation results in Table 3 show a difference of 5.8 %, when comparing simulated data with results obtained experimentally. This difference is due to poor mountings or system imperfections, beyond not rigidity of the lower platform as the simulation determines.

5. Conclusions

By analyzing the data from static simulations, it was possible to determine the strength and deformations that virtual load cells would undergo, as well as to conclude that efforts involved in the force platform when in use are within their nominal values and not cause deformations. From that point, the experimental platform was built and experimental data were compared with the simulation results (the analytical project was not presented in this paper). The dynamic tests by fast Fourier transform (FFT) showed that frequencies values of the vibration modes from the force platform (the range of hundreds Hertz) are outside the usage range (Hertz units), thus problems will not occur in relation to excessive deformations, according to the analyzed oscillatory phenomena.

The signal was treated in a manner that is consistent with acquisition board used in this project. Two gain stages were implemented, resulting in a maximum voltage of 10 V (acquisition board limit) and two 12 dB/octave filter stages to avoid unwanted noises in frequency.

The static calibration of force platform obtained linearity error of 0.49 % on the principal axis (z-axis), representing good functioning of the system. The x and y-axes obtained linearity errors larger than 1.2 % and 1.5 %, respectively, due to imperfections in the calibration methods. Values very close were obtained, comparing simulations with experimental data, showing a difference of 5.8 %.

References

[1]. V. M. Zatsiorsky, Kinematics of human motion, *Human Kinetics,* Champaign, 1998.
[2]. ABNT NBR 5601: 1981, Aços inoxidáveis classificação por composição química (stainless steel), ABNT/CB-28, 1981.
[3]. ABNT 1020, NBR NM87: 2000 (SAE 1020), Aço carbono e ligas para construção mecânica (carbon stell), ABNT, NM 87, 2000.
[4]. C. D. Johnson, Process control instrumentation technology, 5th Edition, *Prentice-Hall*, Upper Saddle River, New Jersey, 1997.
[5]. A. Balbinot, V. J. Brusamarello, Instrumentação e Fundamentos de Medidas (Instrumentation and Measurement Fundamentals), *LTC*, Rio de Janeiro, Vol. 2, 2011.
[6]. OMEGA Engineering INC, The Strain Gage (http://www.omega.com/literature/transactions/volume3/strain.html).
[7]. L. B. Bagesteiro, A. Tamagna, Projeto e Construção de uma Célula de Carga Dinâmica Octogonal, Porto Alegre: DEMEC - UFRGS. 21p, *Caderno Técnico de Engenharia Mecânica*, nº 7, 1995.
[8]. M. A. Urquiza, Desenvolvimento de uma plataforma de Força Multiaxial para Instrumentação Biomédica, *Trabalho de Mestrado Universidade Federal de Uberlândia*, 2005.
[9]. Aluminum Association, Aluminum Standards and Data, 11 ed, *DC,* Washington, 1993.

Guide for Contributors

Aims and Scope

Sensors & Transducers Journal (ISSN 1726-5479) provides an advanced forum for the science and technology of physical, chemical sensors and biosensors. It publishes state-of-the-art reviews, regular research and application specific papers, short notes, letters to Editor and sensors related books reviews as well as academic, practical and commercial information of interest to its readership. Because of it is a peer reviewed international journal, papers rapidly published in *Sensors & Transducers Journal* will receive a very high publicity. The journal is published monthly as twelve issues per year by International Frequency Sensor Association (IFSA). In additional, some special sponsored and conference issues published annually. *Sensors & Transducers Journal* is indexed and abstracted very quickly by Chemical Abstracts, IndexCopernicus Journals Master List, Open J-Gate, Google Scholar, etc. Since 2011 the journal is covered and indexed (including a Scopus, Embase, Engineering Village and Reaxys) in Elsevier products.

Topics Covered

Contributions are invited on all aspects of research, development and application of the science and technology of sensors, transducers and sensor instrumentations. Topics include, but are not restricted to:

- Physical, chemical and biosensors;
- Digital, frequency, period, duty-cycle, time interval, PWM, pulse number output sensors and transducers;
- Theory, principles, effects, design, standardization and modeling;
- Smart sensors and systems;
- Sensor instrumentation;
- Virtual instruments;
- Sensors interfaces, buses and networks;
- Signal processing;
- Frequency (period, duty-cycle)-to-digital converters, ADC;
- Technologies and materials;
- Nanosensors;
- Microsystems;
- Applications.

Submission of papers

Articles should be written in English. Authors are invited to submit by e-mail editor@sensorsportal.com 8-14 pages article (including abstract, illustrations (color or grayscale), photos and references) in both: MS Word (doc) and Acrobat (pdf) formats. Detailed preparation instructions, paper example and template of manuscript are available from the journal's webpage: http://www.sensorsportal.com/HTML/DIGEST/Submition.htm Authors must follow the instructions strictly when submitting their manuscripts.

Advertising Information

Advertising orders and enquires may be sent to sales@sensorsportal.com Please download also our media kit: http://www.sensorsportal.com/DOWNLOADS/Media_Kit_2012.pdf